Rates and Mechanisms of Oxidative Addition to Zerovalent Palladium Complexes Generated *in Situ* from Mixtures of $Pd^0(dba)_2$ and Triphenylphosphine

Christian Amatore,* Anny Jutand,* Fouad Khalil, Mohamed A. M'Barki, and Loïc Mottier

Département de Chimie, Ecole Normale Supérieure, URA CNRS 1679, 24 rue Lhomond, 75231 Paris Cedex 05, France

Received April 14, 1993

The composition of mixtures of $Pd^0(dba)_2$ (dba = dibenzylideneacetone) and triphenylphosphine was examined in THF and DMF, as well as their reactivity *vis à vis* oxidative addition of PhI. It is concluded that, at equilibrium, these catalytic systems contain lesser available amounts of the species active in oxidative addition, *viz.* the low-ligated zerovalent palladium intermediate "$Pd^0(PPh_3)_2$", than $Pd^0(PPh_3)_4$ solutions do for an identical concentration of zerovalent palladium. This arises because, in contradiction with usual assumptions, dba is a better ligand than triphenylphosphine, for the low-ligated active "$Pd^0(PPh_3)_2$", as evidenced by the small values (0.14) of the equilibrium constants of $Pd^0(dba)(PPh_3)_2 + PPh_3 + \text{solvent} \rightleftarrows \text{solvent-}Pd^0(PPh_3)_3 + dba$ in THF or DMF. As a result, oxidative addition of PhI to mixtures of $Pd^0(dba)_2$ and 2 equiv of triphenylphosphine proceeds at an overall rate that is *ca.* 10 times less than that to $Pd^0(PPh_3)_4$. However, it is shown that oxidative addition to the two systems proceeds *via* the same transient intermediate, the solvated low-ligated "$Pd^0(PPh_3)_2$" moiety, evidencing that coordination by dba is not involved in the transition state of oxidative addition. This validates *a posteriori* previous assumptions on such transition states made in the literature, particularly for rationalization of enantiomeric selectivity when chiral phosphines are used.

Introduction

Zerovalent transition metals are versatile reagents prone to activate carbon–halogen or –pseudohalogen bonds through oxidative-addition reactions:[1]

$$R\text{-}X + M^0L_n \rightarrow R\text{-}M^{II}\text{-}L_{n-2}X + 2L \qquad (1)$$

affording organometallic complexes able to undergo a variety of specific reactions.[1,2] For instance, carbon–carbon bonds are easily created by nucleophilic substitution followed by reductive elimination:

$$R\text{-}M^{II}\text{-}L_{n-2}X + Nu^- \xrightarrow{2L} R\text{-}Nu + M^0L_n + X^- \qquad (2)$$

Similarly, electron-transfer activation of the organometallic intermediate allows a polarity inversion that results in a facile reaction with electrophiles:[3]

$$R\text{-}M^{II}\text{-}L_{n-2}X + E^+ \xrightarrow{2e^- + 2L} R\text{-}E + M^0L_n + X^- \qquad (3)$$

It is noteworthy that in most of these reactions the zerovalent transition-metal complexes can be used at catalytic concentrations, since they are regenerated after the reductive-elimination steps. For example, zerovalent palladium complexes are efficient catalysts in synthetic reactions involving aryl or vinyl halides, aryl or vinyl triflates, allylic acetates or carbonates, *etc.*[2] These complexes are easily available and usable in their stable chemical form, Pd^0L_4, e.g. $Pd^0(PPh_3)_4$.[2] Yet, it has been established that the active catalytic species is the low-ligated moiety, Pd^0L_2, formed upon deligation of the precursor complex:[4]

$$Pd^0L_4 \rightleftarrows Pd^0L_3 + L \qquad K \gg 1\ M \qquad (4)$$

$$Pd^0L_3 \rightleftarrows Pd^0L_2 + L \qquad K' \ll 1\ M \qquad (5)$$

The large overall endergonicity of the second step results in the fact that Pd^0L_2, the "true" active catalyst, is often present at trace levels, with the obvious consequence that the kinetics of the chain propagation may be too slow. To prevent such inconvenience, several methods have been proposed for the generation *in situ* of the active moiety Pd^0L_2. For example, this species can be generated upon the stoichiometric two-electron overall reduction of a stable precursor, *viz.* the divalent complex $Pd^{II}L_2X_2$:

$$Pd^{II}L_2X_2 + 2e^- \rightarrow Pd^0L_2 + 2X^- \qquad (6)$$

This reduction can be performed homogeneously[5-7] in the reaction mixture by a Grignard reagent or an organometal species (*i.e.*, the nucleophile in eq 2) or by electrochemical means.[8] Similarly, we have recently established that the method which consists of using palladium(II) diacetate in

* To whom all correspondence should be addressed.

(1) For a comprehensive review and discussion of oxidative addition see *e.g.*: Kochi, J. K. In *Organometallic Mechanisms and Catalysis*; Academic Press: New York, 1978; Part I, Chapter 7.

(2) For reviews, see: (a) Heck, R. F. *Acc. Chem. Res.* **1979**, *12*, 146. (b) Heck, R. F. *Org. React.* **1979**, *27*, 345. (c) Kumada, M. *Pure Appl. Chem.* **1980**, *52*, 669. (d) Tsuji, J. *Organic Synthesis via Palladium Compounds*; Springer-Verlag: New York, 1980. (e) Negishi, E. I. *Acc. Chem. Res.* **1982**, *15*, 340. (f) Heck, R. F. *Palladium in Organic Synthesis*; Academic Press, New York, 1985. (g) Stille, J. K. *Angew. Chem., Int. Ed. Engl.* **1986**, *25*, 508.

(3) For nickel-centered catalysts see *e.g.*: (a) Colon, I.; Kelsey, D. R. *J. Org. Chem.* **1986**, *51*, 2627. (b) Amatore, C.; Jutand, A. *Organometallics* **1988**, *7*, 2203. (b) Amatore, C.; Jutand, A. *J. Am. Chem. Soc.* **1991**, *113*, 2819. (c) Amatore, C.; Jutand, A.; Mottier, L. *J. Electroanal. Chem. Interfacial Electrochem.* **1991**, *306*, 125. (d) Amatore, C.; Jutand, A. *J. Electroanal. Chem. Interfacial Electrochem.* **1991**, *306*, 141. (e) Fox, M. A.; Chandler, D. A.; Lee, C. *J. Org. Chem.* **1991**, *56*, 3246. For palladium-centered catalysts, see *e.g.*: (f) Torii, S.; Tanaka, H.; Morisaki, K. *Tetrahedron Lett.* **1985**, *26*, 1655. (g) Torii, S.; Tanaka, H.; Hamatani, T.; Morisaki, K.; Jutand, A.; Pflüger, F.; Fauvarque, J. F. *Chem. Lett.* **1986**, 169. (h) Amatore, C.; Jutand, A.; Khalil, F.; Nielsen, M. *J. Am. Chem. Soc.* **1991**, *114*, 7076.

(4) (a) Fauvarque, J. F.; Pflüger, F.; Troupel, M. *J. Organomet. Chem.* **1979**, *208*, 419. (b) Amatore, C.; Pflüger, F. *Organometallics* **1990**, *9*, 2276. For a similar situation for $Ni^0(PR_3)_4$, compare: (c) Elson, I. E.; Morrell, D. G.; Kochi, J. K. *J. Organomet. Chem.* **1975**, *84*, C7. (d) Tsou, T. T.; Kochi, J. K. *J. Am. Chem. Soc.* **1979**, *101*, 6319.

0276-7333/93/2312-3168$04.00/0 © 1993 American Chemical Society

the presence of phosphines also amounts to the generation of Pd^0L_2, *via* an overall two-electron inner-sphere reduction of the palladium center by 1 equiv of phosphine:[9]

$$Pd^{II}(OAc)_2 + 3PPh_3 \rightarrow Pd^0(PPh_3)_2 + O{=}PPh_3 + etc. \quad (7)$$

In this paper we wish to discuss a third method that has been adopted by several groups in the last 10 years. It consists of introducing zerovalent palladium in the form of $Pd^0(dba)_2$ (dba = dibenzylideneacetone) in the presence of phosphine ligands.[10,11] Interest in such a method is based on the assumption that dba, being a weaker ligand than phosphine, should be easily removed from the palladium center to afford the active species Pd^0L_2 in nearly stoichiometric amounts:

$$Pd^0(dba)_2 + 2L \rightleftharpoons Pd^0L_2 + 2dba \quad (8)$$

Moreover, the method presents the two following important advantages for synthetic chemistry. First, $Pd^0(dba)_2$ is insensitive to oxygen; therefore, its storage and manipulation do not require special care, in contrast *e.g.* with the usual catalyst $Pd^0(PPh_3)_4$. Second, whenever the ligand exchange in eq 8 occurs in the reaction mixture in the presence of only 2 equiv of phosphine, a variety of expensive phosphine ligands can be used at will, an obvious advantage for the generation *in situ* of catalysts with chiral properties.[10i,l,m,s,t]

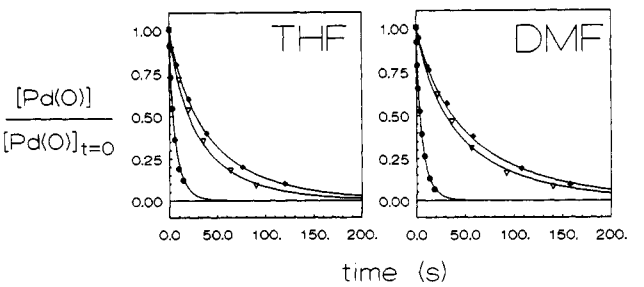

Figure 1. Kinetics of oxidative addition of PhI to $Pd^0(PPh_3)_4$ (●), $Pd^0(dba)_2$ with 2 equiv of PPh_3 (▽), or $Pd^0(dba)_2$ with 4 equiv of PPh_3 (◆), in THF or in DMF. For each system presented the initial concentration in palladium(0) complex is 2 mM, and the medium contains n-Bu_4NBF_4 (0.3 M) at 20 °C.

However, there are several indications in the literature that the process in eq 8 is oversimplified, if not inaccurate. Indeed, if eq 8 were entirely correct, the catalytic properties of $Pd^0(dba)_2$ in the presence of 4 equiv of PPh_3 would be identical with those of $Pd^0(PPh_3)_4$. However, the latter appears to be often a more efficient catalyst than $Pd^0(dba)_2$ in the presence of 4 equiv of PPh_3, and, under some circumstances, even more reactive than $Pd^0(dba)_2$ in the presence of 2 equiv of PPh_3.[11h,j,k,o,s] Such observations taken from the literature are clearly related to the ease of the oxidative-addition step in eq 1, as established by the results reported in Figure 1. Indeed, this figure compares the reactivities of $Pd^0(PPh_3)_4$, $Pd^0(dba)_2 + PPh_3$ (4 equiv), and $Pd^0(dba)_2 + PPh_3$ (2 equiv) in the presence of 5 equiv of PhI. It shows that the overall rate of oxidative addition to $Pd^0(PPh_3)_4$ is *ca.* 4–5 times faster than that to $Pd^0(dba)_2$ + 2 equiv of PPh_3, and *ca.* 6–7 times faster than that to $Pd^0(dba)_2$ + 4 equiv of PPh_3, as easily found by comparing the half-lives of the three systems.

Such results clearly evidence that dba does not play an innocent role in the system, as implicitly suggested by the formulation in eq 8. Owing to the increased importance of this method in synthetic chemistry,[10,11] this prompted us to undertake a detailed study of the reactivity of catalystic systems consisting of mixtures of $Pd^0(dba)_2$ and triphenylphosphine, so as to compare their properties with those of $Pd^0(PPh_3)_4$ or of other precursors of "$Pd^0(PPh_3)_2$". We wish to present here the results of this study.

(5) For Nu^- as the reducing agent see e.g.: (a) Fauvarque, J. F.; Jutand, A. *Bull. Soc. Chim. Fr.* **1976**, 765. (b) Hayashi, T.; Konishi, M.; Kumada, M. *Tetrahedron Lett.* **1979**, 1871. (c) Milstein, D.; Stille, J. K. *J. Am. Chem. Soc.* **1979**, *101*, 4992. (d) Minato, A.; Tamao, K.; Hayashi, T.; Suzuki, K.; Kumada, M. *Tetrahedron Lett.* **1980**, 845. (e) Minato, A.; Tamao, K.; Hayashi, T.; Suzuki, K.; Kumada, M. *Tetrahedron Lett.* **1981**, 5319. (f) Hayashi, T.; Konishi, M.; Kobori, Y.; Kumada, M.; Higushi, T.; Hirotsu, K. *J. Am. Chem. Soc.* **1984**, *106*, 158. (g) Uno, M.; Seto, K.; Ueda, W.; Masuda, M.; Takahashi, S. *Synthesis* **1985**, 506.

(6) For reduction by an organometal see e.g.: (a) Kosugi, M.; Shimizu, T.; Migita, T. *Chem. Lett.* **1978**, 13. (b) King, A. O.; Negishi, E. I.; Villani, F. J.; Silveria, A., Jr. *J. Org. Chem.* **1978**, *43*, 358. (c) Negishi, E. I.; Okukado, N.; King, A. O.; van Horn, D. E.; Spiegel, B. I. *J. Am. Chem. Soc.* **1978**, *100*, 2254. (d) Urata, H.; Suzuki, H.; Moro-oka, Y.; Ikawa, T. *J. Organomet. Chem.* **1989**, *364*, 235. For ^{31}P NMR identification of the low-ligated palladium(0) species formed stoichiometrically under such conditions, see: (e) Negishi, E. I.; Takahashi, T.; Akiyoshi, K. *J. Chem. Soc., Chem. Commun.* **1986**, 1338.

(7) Another interesting approach consists of introducing the transition-metal catalyst under the form of the organometallic derivative $Ar{-}Pd^{II}L_2X$ formed independently (*via* eq 1). Compare e.g.: (a) Fauvarque, J. F.; Jutand, A. *J. Organomet. Chem.* **1979**, *177*, 273. (b) Milstein, D.; Stille, J. K. *J. Am. Chem. Soc.* **1979**, *101*, 4992. (c) Sekiya, A.; Ishikawa, N. *J. Organomet. Chem.* **1976**, *118*, 349.

(8) (a) Amatore, C.; Azzabi, M.; Jutand, A. *J. Am. Chem. Soc.* **1991**, *113*, 1670. (b) Amatore, C.; Azzabi, M.; Jutand, A. *J. Am. Chem. Soc.* **1991**, *113*, 8375.

(9) Amatore, C.; Jutand, A.; M'Barki, M. A. *Organometallics* **1992**, *11*, 3009.

(10) For the use of $Pd(dba)_2$ with bidentate ligands, see: (a) Fiaud, J. C.; Hibon de Gournay, A.; Larchevêque, M.; Kagan, H. B. *J. Organomet. Chem.* **1978**, *154*, 175. (b) Fiaud, J. C.; Malleron, J. L. *Tetrahedron Lett.* **1980**, *21*, 4437. (c) Fiaud, J. C.; Malleron, J. L. *J. Chem. Soc., Chem. Commun.* **1981**, 1159. (d) Julia, M.; Nel, M.; Righini, A.; Ugen, D. *J. Organomet. Chem.* **1982**, *235*, 113. (e) Ahmar, M.; Cazes, B.; Goré, J. *Tetrahedron Lett.* **1984**, *25*, 4505. (f) Ahmar, M.; Cazes, B.; Goré, J. *Tetrahedron Lett.* **1985**, *26*, 3795. (g) Rajanbabu, T. V. *J. Org. Chem.* **1985**, *50*, 3642. (h) Fiaud, J. C.; Denner, B.; Malleron, J. L. *J. Organomet. Chem.* **1985**, *291*, 393. (i) Genet, J. P.; Férroud, D.; Jugé, S.; Ruiz Montès, J. *Tetrahedron Lett.* **1986**, *27*, 4573. (j) Fiaud, J. C.; Legros, J. Y. *J. Org. Chem.* **1987**, *52*, 1907. (k) Bäckwall, J. E.; Vagberg, J. E.; Zercher, C.; Genet, J. P.; Denis, A. *J. Org. Chem.* **1987**, *52*, 5430. (l) Genet, J. P.; Jugé, S.; Ruiz Montès, J.; Gaudin, J. M. *J. Chem. Soc., Chem. Commun.* **1988**, 718. (m) Fiaud, J. C.; Legfos, J. Y. *Tetrahedron Lett.* **1988**, *29*, 2959. (n) Genet, J. P.; Uziel, J.; Jugé, S. *Tetrahedron Lett.* **1988**, *29*, 4559. (o) Fournet, G.; Balme, G.; Barrieux, J. J.; Goré, J. *Tetrahedron* **1988**, *44*, 5821. (p) Alper, H.; Saldana-Maldonado, M.; Lin, I. J. B. *J. Mol. Catal.* **1988**, *49*, L27. (q) Lin, I. J. B.; Alper, H. *J. Chem. Soc., Chem. Commun.* **1989**, *4*, 248. (r) Susuki, O.; Inoue, S.; Sato, K. *Bull. Chem. Soc. Jpn.* **1989**, *62*, 239. (s) Fiaud, J. C.; Legros, J. Y. *J. Organomet. Chem.* **1989**, *370*, 383. (t) Fiaud, J. C.; Legros, J. Y. *J. Org. Chem.* **1990**, *55*, 4840. (u) Chaptal, N.; Colovray-Gotteland, V.; Grandjean, C.; Cazes, B.; Goré, J. *Tetrahedron Lett.* **1991**, *32*, 1795. (v) El Ali, B.; Alper, H. *J. Org. Chem.* **1991**, *56*, 5357.

(11) For the use of $Pd(dba)_2$ with monodentate ligands, see: (a) Inoue, Y.; Hibi, T.; Satake, M.; Hashimoto, H. *J. Chem. Soc., Chem. Commun.* **1979**, 982. (b) Balavoine, G.; Eskenazi, C.; Guillemont, M. *J. Chem. Soc., Chem. Commun.* **1979**, 1109. (c) Binger, P.; Schuchardt, U. *Chem. Ber.* **1980**, *113*, 1063. (d) Binger, P.; McMeeking, J.; Schuchardt, U. *Chem. Ber.* **1980**, *113*, 2372. (e) Binger, P.; Schuchardt, U. *Chem. Ber.* **1980**, *113*, 3033. (f) Fiaud, J. C.; Malleron, J. L. *Tetrahedron Lett.* **1980**, *21*, 4437. (g) Binger, P.; Schuchardt, U. *Chem. Ber.* **1981**, *114*, 1649. (h) Russell, C. E.; Hegedus, L. S. *J. Am. Chem. Soc.* **1983**, *105*, 943. (i) Sheffy, F. K.; Stille, J. K. *J. Am. Chem. Soc.* **1983**, *105*, 7173. (j) Henin, F.; Pete, J. P. *Tetrahedron Lett.* **1983**, *24*, 4687. (k) Ferroud, D.; Genet, J. P.; Muzart, J. *Tetrahedron Lett.* **1984**, *25*, 4379. (l) Sheffy, F. K.; Godschalx, J. P.; Stille, J. K. *J. Am. Chem. Soc.* **1984**, *106*, 4833. (m) Inoue, Y.; Ohtsuka, Y. M.; Hashimoto, H. *Bull. Chem. Soc. Jpn.* **1984**, *57*, 3345. (n) Inoue, Y.; Toyofuku, M.; Taguchi, M.; Okada, S. I.; Hashimoto, H. *Bull. Chem. Soc. Jpn.* **1986**, *59*, 885. (o) Oppolzer, W.; Gaudin, J. M. *Helv. Chim. Acta* **1987**, *70*, 1477. (p) Oppolzer, W.; Swenson, R. E.; Gaudin, J. M. *Tetrahedron Lett.* **1988**, *29*, 5529. (q) Genet, J. P.; Jugé, S.; Achi, S.; Mallart, S.; Ruiz Montés, J.; Levif, G. *Tetrahedron* **1988**, *44*, 5263. (r) Farina, V.; Baker, S. R.; Benigni, D. A.; Sapino, C., Jr. *Tetrahedron Lett.* **1988**, *29*, 5739. (s) Murahashi, S. I.; Taniguchi, Y.; Imada, Y.; Tanigawa, Y. *J. Org. Chem.* **1989**, *54*, 3292. (t) Legros, J. Y.; Fiaud, J. C. *Tetrahedron Lett.* **1990**, *31*, 7453.

Results

^{31}P NMR Study of Mixtures of $Pd^0(dba)_2$ and Triphenylphosphine or of $Pd^0(PPh_3)_4$ and dba in THF or DMF. In the presence of 1 or 2 equiv of PPh_3, the ^{31}P NMR spectrum of $Pd^0(dba)_2$ in THF consists of a sharp doublet at δ 25.06 and 26.95 ppm (*vs* H_3PO_4), showing that a single species is formed that contains two nonequivalent phosphines. It is noteworthy that when 10 equiv of PhI is added to this mixture, the above doublet disappears and is replaced by a common signal at 24.50 ppm characteristic of $Ph-Pd^{II}I(PPh_3)_2$.[12] This establishes that the doublet corresponds to a zerovalent palladium species bearing two chemically inequivalent phosphines: $Pd^0(dba)_n(PPh_3)_2$, with $1 \leq n \leq 2$. ^{1}H NMR of the same solution shows that stoichiometric amounts of free dba are present in the medium under these conditions; from this we conclude that $n = 1$:[13]

$$Pd^0(dba)_2 + 2PPh_3 \rightarrow Pd^0(dba)(PPh_3)_2 + dba \qquad (9)$$

When 1 or 2 equiv more of phosphine is added to this solution, the doublet for $Pd^0(dba)(PPh_3)_2$ is still observed, although of decreased intensity, but a broad signal develops upfield (δ 1.79 ppm for 4 equiv of PPh_3) in the range where the resonance for $Pd^0(PPh_3)_4$ alone is observed under the same conditions (δ 0.9 ppm).[14,15] Increasing the concentration of phosphine results in a progressive decay of the doublet and in an increase of the intensity of the broad signal that narrows and moves continuously upfield (*e.g.* δ −0.96 ppm for 10 equiv of PPh_3), to tend ultimately toward the signal observed for a free phosphine (δ −5.25 ppm).[14] It is noteworthy that in each case the NMR spectrum is independent of time. Therefore, the above data suggest that, in the presence of additional equivalents of phosphines, $Pd^0(dba)(PPh_3)_2$ is involved in a succession of equilibria that lead ultimately to the same species that are generated from $Pd^0(PPh_3)_4$ (see eqs 4 and 5) in the presence of identical excesses of phosphine:[15]

$$Pd^0(dba)(PPh_3)_2 \underset{dba}{\overset{2PPh_3}{\rightleftarrows}} Pd^0(PPh_3)_4 \rightleftarrows etc. \qquad (10)$$

To test for the effectiveness of the above equilibrium, the ^{31}P NMR spectrum of $Pd^0(PPh_3)_4$ was determined in the presence of different excesses of dba. This led to the observation of spectra very reminiscent of those obtained from mixtures of $Pd^0(dba)_2$ and PPh_3. For example, for 4 equiv of dba, one observes the doublet at 25.06 and 26.95 ppm, characteristic of $Pd^0(dba)(PPh_3)_2$, and a broad signal at 1.07 ppm, featuring PPh_3 as involved in the rapid equilibria in eqs 4 and 5.[14]

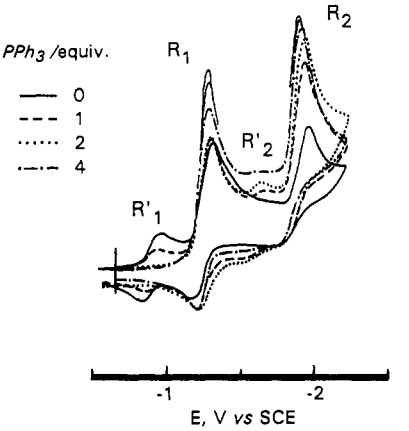

Figure 2. Voltammetric reduction of $Pd^0(dba)_2$, 2 mM in THF/*n*-Bu_4NBF_4 (0.3 M), in the presence of various equivalents of PPh_3 added, as shown in the insert. Conditions: gold-disk electrode (0.5-mm diameter); scan rate 0.2 V·s^{-1}; 20 °C. For the sake of clarity only the peak sections of waves R_1 and R_2 are shown for 6 and 8 equiv of added phosphine.

All these results remain essentially identical when the NMR studies are performed in DMF, except for slight variations of the chemical shifts of the various species identified above.[16]

Cyclic Voltammetry Investigation in Reduction. The above results are confirmed independently by cyclic voltammetry in both solvents. Indeed, reduction of $Pd^0(dba)_2$ alone in DMF or THF gives a set of two reduction waves, R_1 and R_2 in Figure 2,[17] that are characteristic of the reduction of free dba as established by cyclic voltammetry of an authentic sample of the latter. The current intensities of waves R_1 and R_2 establish that 1 equiv of free dba is produced upon dissolution of $Pd^0(dba)_2$ in THF or DMF:[18]

$$Pd^0(dba)_2 \rightarrow Pd^0(dba) + dba \qquad (11)$$

The validity of this formulation is independently confirmed by the results of ^{1}H NMR performed on the same solutions, which establish also the liberation of 1 equiv of dba upon dissolution of $Pd^0(dba)_2$ in THF or DMF in the concentration range investigated.

When PPh_3 is added to these solutions, one still observes the two main reduction waves, R_1 and R_2, featuring the reduction of free dba, except that now their current intensities increase to double eventually at large excesses of phosphine (*e.g.* for $[PPh_3]/[Pd^0(dba)_2] \geq 6$ in DMF or 8 in THF, at 0.2 V·s^{-1}). This result, which agrees with the formulation in eq 10, evidences that up to 2 equiv of dba is released in the medium in the presence of large excesses of PPh_3.

For small excesses of phosphine added, a set of two smaller additional waves, R'_1 and R'_2, are also observed

(12) Compare refs 6e and 8b. In DMF $Ph-Pd^{II}I(PPh_3)_2$ gives a thin singlet at δ 23.39 ppm.

(13) This is in agreement with previous results obtained with other phosphine ligands; see: Huser, M. Ph.D. Dissertation, University Louis Pasteur, Strasbourg, France, 1988. In this work, it is shown, on the basis of an IR study, that a single dba ligand is unsymmetrically coordinated to the palladium center, *via* one of its carbon–carbon double bonds. This dissymmetry results in the nonequivalence of the two phosphorus atoms.

(14) (a) Compare ref 8b. (b) This single signal corresponds to the species involved in the rapid equilibria in eqs 4 and 5 and is therefore strongly dependent on the excess of free phosphine. As expected, increasing the excess of PPh_3 results in a progressive narrowing and shift of this signal so as to feature the resonance of the free phosphine at δ −5.25 ppm in THF.

(15) The fact that the signal due to $Pd^0(dba)(PPh_3)_2$ remains unchanged, except for its intensity, shows that any equilibria possibly involving this species and any other species formed in the presence of excess phosphine (*vide infra*) are slow within the time scale of ^{31}P NMR (162 MHz).

(16) ^{31}P NMR in DMF: $Pd^0(dba)(PPh_3)_2$, doublet at δ 25.29 and 27.19 ppm (J_{PP} was too small *vis à vis* the half-widths of the peaks—*ca.* 28 Hz—to be determined); $Pd^0(PPh_3)_4$ (20 mM, alone), broad signal at δ 9 ppm; free PPh_3, singlet at δ −5.41 ppm; $Ph-Pd^{II}I(PPh_3)_2$, singlet at δ 23.39 ppm.

(17) In THF at 0.2 V·s^{-1}, at $E^p_{R_1} = -1.29$ (partially chemically reversible) and $E^p_{R_2} = -2.0$ V *vs* SCE (chemically irreversible); in DMF at 0.2 V·s^{-1}, at $E^p_{R_1} = -1.29$ (partially chemically reversible) and $E^p_{R_2} = -2.0$ V *vs* SCE (chemically irreversible).

(18) However, it is not clear if $Pd^0(dba)$ is a monomer, as suggested by the formulation in eq 11, or rather corresponds to a species coordinated by the solvent or aggregates thereof. Under different experimental conditions (^{1}H NMR in $CDCl_3$) we observed the release of $^1/_2$ equiv of dba per palladium with simultaneous formation of $(Pd^0)_2(dba)_3$. For isolation and characterization of $(Pd^0)_2(dba)_3(CHCl_3)$ see: Ukai, T.; Kawazura, H.; Ishii, Y.; Bonnet, J. J.; Ibers, J. A. *J. Organomet. Chem.* **1974**, *65*, 253.

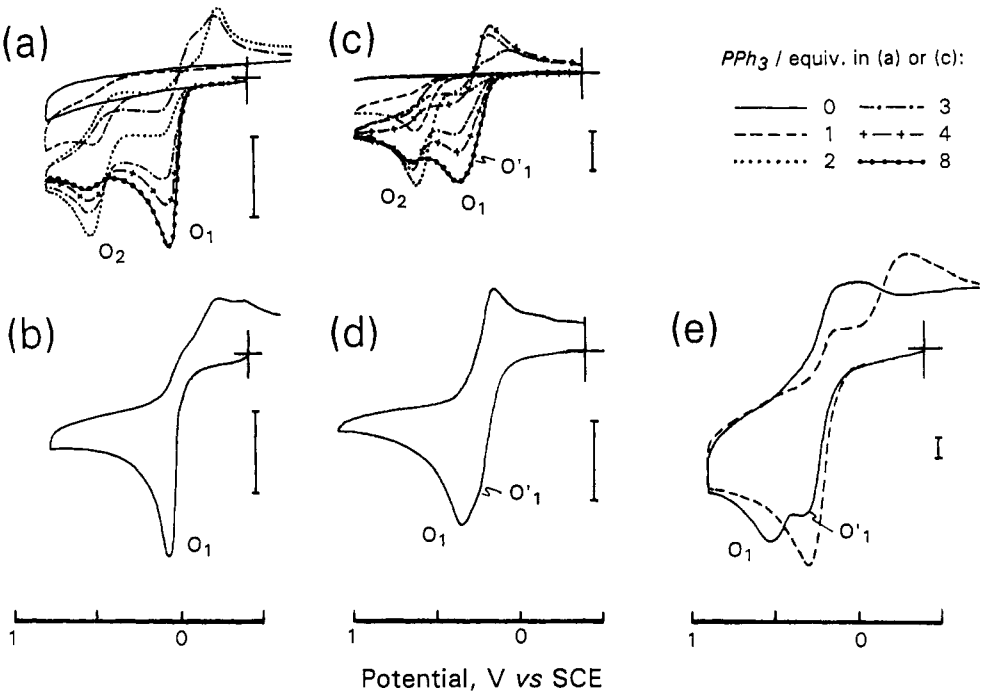

Figure 3. (a,c) Voltammetric oxidation of $Pd^0(dba)_2$ (2 mM) in the presence of various equivalents of PPh_3 added, as shown in the insert (scan rate 0.2 $V \cdot s^{-1}$). For the sake of clarity only the foward scans are shown for 4 and 8 equiv of added phosphine. (b,d) Voltammetry of $Pd^0(PPh_3)_4$ (2 mM) at 0.2 $V \cdot s^{-1}$. (e) Voltammetry of $Pd^0(PPh_3)_4$ (2 mM) at 5 $V \cdot s^{-1}$ alone (solid curve) or in the presence of added DMF (4% v/v) (dashed curve). Solvent: (a,c) DMF/*n*-Bu_4NBF_4 (0.3 M); (b,d,e) THF/*n*-Bu_4NBF_4 (0.3 M). Conditions: gold-disk electrode (0.5-mm diameter); 20 °C. The vertical bar shown for each set represents 0.5 μA.

$$Pd^0(dba) \xrightarrow{2PPh_3} Pd^0(dba)(PPh_3)_2 \underset{dba}{\overset{2PPh_3}{\rightleftharpoons}} Pd^0(PPh_3)_4 \rightleftharpoons \text{etc.} \quad (12)$$

as illustrated in Figure 2. The current intensity of wave R'_1 is maximum (*viz.* less than 20% of that of R_1) in the absence of added phosphine. It is divided by 2 in the presence of 1 equiv of phosphine and totally disappears for 2 equiv. This wave can therefore be ascribed to the reduction of dba coordinated to the palladium(0) center in $Pd^0(dba)$.[19] Wave R'_2 does not appear in the absence of added phosphine, and its current intensity passes through a maximum (at less than 10% of that of R_1) for 2 equiv of phosphine; it becomes negligible for more than 4 equiv of added phosphine. A secure assignment of this wave was not possible. However, it may be tentatively ascribed to the reduction of dba coordinated to a zerovalent palladium center formed intermediately during the first steps (left-hand side) of the process in eq 12.

Finally, it is important to emphasize that the system of waves represented in Figure 2 is independent of the time elapsed since the preparation of the solution (*viz.* from a few minutes at least, up to 2 h at maximum), showing that the solution does not evolve from its equilibrium achieved upon mixing. However, the shapes of waves and their current intensities depend on the value of the scan rate used ($50 \geq v \geq 0.1$ $V \cdot s^{-1}$). Such a characteristic behavior shows that the amount of "free" dba, as reflected by the magnitudes of waves R_1 and R_2, does not represent a true equilibrium concentration but rather a "dynamic" concentration due to the partial displacement of the labile equilibrium in eq 10 toward its right-hand side.[20-22] This occurs because of the continuous reduction of dba occurring at the electrode surface when the voltammetric scan is performed. In particular this demonstrates that the quantities of dba released in the solution are less than they may appear from the magnitudes of the waves in Figure 2.[20,21] In other words, this establishes that a large excess of phosphine is required to deligate completely both dba ligands from the palladium center, in opposition with former implicit formulations (eq 8).

Cyclic Voltammetry Investigation in Oxidation. Oxidation of mixtures of $Pd^0(dba)_2$ and PPh_3 ($\geq$2 equiv)[19] in DMF shows two waves, O_1 and O_2, as illustrated in Figure 3a.[23] Wave O_1, being identical with that observed upon oxidation of an authentic sample of $Pd^0(PPh_3)_4$ in DMF (compare Figure 3b), features the overall two-electron oxidation of $Pd^0(PPh_3)_3$,[24] presumably coordinated or strongly solvated by a solvent molecule (denoted as *S*-$Pd^0(PPh_3)_3$ in the following; *vide infra*). The second wave, O_2, is fully developed only when 2 equiv of phosphine is used. By comparison to the above results of ^1H and ^{31}P NMR, we ascribe this wave to the oxidation of $Pd^0(dba)(PPh_3)_2$, the main species present in the medium for 2 equiv of phosphine added. In agreement with these attributions, the variations of the respective magnitudes of the current intensities of waves O_1 and O_2, as a function

(19) (a) This attribution is further supported by the simultaneous observation of an oxidation wave at E^p = 1.26 V *vs* SCE (in THF), whose current intensity is exactly twice that of wave R_1. We ascribe this oxidation wave to the two-electron oxidation of $Pd^0(dba)$. The fact that wave R_1 is well-shaped indicates that the reaction between $Pd^0(dba)$ and PPh_3 (left-hand side of eq 12) is irreversible or is a very slow equilibrium if reversible (*vide infra* and refs 20 and 21). (b) In THF or DMF at 0.2 $V \cdot s^{-1}$, at $E^p_{R'_1}$ = −0.94 (chemically reversible) and $E^p_{R'_2}$ = −1.59 V *vs* SCE (chemically irreversible).

(20) Bard, A. J.; Faulkner, L. R. *Electrochemical Methods*; Wiley: New York, 1980; pp 443-449.

(21) (a) Savéant, J. M.; Vianello, E. *Electrochim. Acta* **1963**, *8*, 905. (b) Nicholson, R. S.; Shain, I. *Anal. Chem.* **1964**, *36*, 706.

(22) It is worth emphasizing that the equilibrium in eq 13 (or the left-hand-side equilibrium in eq 10) is slow enough to be "frozen" on the NMR time scales but is labile on the voltammetric time scale considered here (*vide infra*).

(23) In DMF at 0.2 $V \cdot s^{-1}$, E^p = 0.14 (O_1), 0.56 (O_2) V *vs* SCE; in THF at 0.2 $V \cdot s^{-1}$, E^p = 0.37 (O_1), 0.30 (O'_1, shoulder), 0.64 (O_2) V *vs* SCE.

of the number of equivalents of added phosphine, roughly parallel those described above for the ^{31}P NMR spectra of the same solutions. However, it must be emphasized that these respective magnitudes are scan rate dependent, evidencing that the equilibrium existing between these species is a dynamic equilibrium, prone to be displaced when the voltammogram is performed.[20,21] This is particularly apparent in the voltammogram reported in Figure 3a for 2 equiv of phosphine. Thus, wave O_1 does not present the characteristic shape of a voltammogram but is instead "plateau shaped", a characteristic signature for the occurrence of a CE electrochemical mechanism[20-22]

$$Pd^0(dba)(PPh_3)_2 + PPh_3 \overset{S}{\rightleftarrows} S\text{-}Pd^0(PPh_3)_3 + dba \quad (13)$$

$$S\text{-}Pd^0(PPh_3)_3 - 2e^- \rightarrow etc. \qquad \text{wave } O_1 \quad (14)$$

$$Pd^0(dba)(PPh_3)_2 - 2e^- \rightarrow etc. \qquad \text{wave } O_2 \quad (15)$$

in which the equilibrium in eq 13 lying to its left-hand side (because of the lack in phosphine) is continuously displaced by the electrochemical consumption of S-$Pd^0(PPh_3)_3$ at the electrode surface (eq 14) when wave O_1 is scanned. Note that such a pattern is in complete agreement with that observed in reduction, since then the equilibrium in eq 13 is displaced by reduction of dba.

In THF, one observes essentially the same behavior.[23,24] The only critical difference between the two solvents is that in THF, at slow scan rates, wave O_1 appears broader than in DMF, presenting a shoulder (noted O'_1) on the rising portion of the voltammetric peak, as shown in Figure 3c.[23] The same voltammetric pattern (*viz.* the two overlapping waves O_1 and O'_1) is observed for an authentic solution of $Pd^0(PPh_3)_4$ in THF (compare Figure 3d), showing that two oxidizable species coexist in such solutions: that oxidized at the shoulder (O'_1) and that oxidized at the main peak (O_1). These two species are in rapid equilibrium within the time scale of cyclic voltammetry at slow scan rates ($v \leq 0.5$ V·s^{-1}). However, at faster scan rates ($v \geq 5$ V·s^{-1}), *viz.* on shorter time scales, this equilibrium tends to be "frozen", as evidenced in Figure 3e (solid curve). These two species can be tentatively described as S-$Pd^0(PPh_3)_3$ and $Pd^0(PPh_3)_3$:

$$Pd^0(PPh_3)_3 \overset{S}{\rightleftarrows} S\text{-}Pd^0(PPh_3)_3 \qquad K_S \quad (16)$$

In DMF, a better ligand than THF, this equilibrium is totally displaced toward S-$Pd^0(PPh_3)_3$, leading to the observation of the single well-defined wave O_1. Our former attribution of wave O_1 to the oxidation of S-$Pd^0(PPh_3)_3$ in DMF, rather than to that of $Pd^0(PPh_3)_3$, is partially based on this observation. This can be further substantiated by the following result. When DMF is added to a solution of $Pd^0(PPh_3)_4$ in THF, the well-resolved system of the two waves O_1 and O'_1 observed in pure THF at fast scan rates is progressively replaced by a single oxidation wave, at a potential slightly less positive than that of O'_1 (Figure 3e, dashed curve). This behavior shows that a DMF molecule may interact with the palladium(0) center sufficiently strong to affect its redox behavior,[24c] even when the DMF concentration in THF is small. From this we conclude *a fortiori* that a DMF molecule is also coordinated to the palladium(0) center in pure DMF solutions.

Chronoamperometric Investigation. The quantitation of the above process (eqs 13–15), possibly complicated in THF by the additional involvement of the equilibrium in eq 16, is formally possible from voltammograms such as those presented in Figure 3a,c. However, the shapes of the voltammetric waves strongly depend on the exact chemical sequence initiated by the initial electron exchange at the electrode. Since these mechanisms are presently unknown for the oxidations occurring at waves O_1 (and O'_1 in THF) or O_2,[24] a quantification of the processes at hand was unfortunately impossible on the basis of cyclic voltammetry only. To avoid this difficulty, we resorted to chronoamperometry. Indeed, in chronoamperometry, the current corresponding to a potential step performed on the plateau of a wave is independent of the exact chemical sequence initiated by the initial electron exchange at the electrode surface but depends only on the overall number of electrons exchanged.

Figure 4a presents the result of such an investigation in THF, in the form of a plot of $I_\theta = [i_E(\theta)]\theta^{1/2}$,[25] as a function of the step potential E, where $i_E(\theta)$ is the current measured at time θ after a potential E has been applied to the working electrode. This figure shows that three waves are observed at short pulse duration (θ = 20 ms), whose half-wave potentials correspond to waves O'_1, O_1, and O_2 observed in cyclic voltammetry. In DMF the situation is analogous yet slightly simplified because wave O'_1 is not observed. In both solvents, the respective size of these waves depends on the duration θ of the potential step, as well as on the quantity of added phosphine, as evidenced by the variations of the chronoamperometric polarogram in Figure 4a. These variations can be quantified by monitoring the variations of the current plateaus of the three (THF) or two (DMF) waves as a function of the pulse duration θ. This is represented for DMF in Figure 4b under the form of the variations of $R_\theta = I_\theta^1/(I_\theta^1 + I_\theta^2)$. It is noteworthy that if more than 2 equiv of phosphine is used, the quantity $(I_\theta^1 + I_\theta^2)/C^0$, where C^0 is the concentration of $Pd^0(dba)_2$ introduced in the cell, is independent of θ or of the exact amount of phosphine. This result establishes that the two oxidation waves O_1 and O_2 correspond altogether to the two-electron oxidation of the overall palladium(0) present in the cell, irrespective of its exact coordination shell.[24] In other words, this confirms the results implicitly assumed above in the description of voltammetric experiments in DMF: (i) that waves O_1 and O_2 represent the respective two-electron oxidations of S-$Pd^0(PPh_3)_3$ and of $Pd^0(dba)(PPh_3)_2$ and (ii) that these two species in equilibrium (eq 13) are the only species present in solution at significant concentrations in mixtures of $Pd^0(dba)_2$ and PPh_3, when more than 2 equiv of phosphine is added.

In THF, the situation is slightly more complex because, as noticed above in cyclic voltammetry, the first oxidation wave (*viz.* the counterpart of wave O_1 in DMF) does not represent a single oxidative process but is the result of the

(24) (a) The electron stoichiometries of the processes occurring at waves O_1 and O_2 (in DMF) or O_1, O'_1, and O_2 (in THF) could not be determined independently, because of the involvement of the CE processes described in the text. However, the sum of the oxidation currents of these waves, as determined by chronoamperometry on the plateau of wave O_2 (*vide infra*), corresponds to an overall two-electron process per zerovalent palladium center: $n = 1.9 \pm 0.2$. This absolute electron stoichiometry was determined by following the procedure described in: (b) Amatore, C.; Azzabi, M.; Calas, P.; Jutand, A.; Lefrou, C.; Rollin, Y. *J. Electroanal. Chem. Interfacial Electrochem.* **1990**, *288*, 45. (c) The electrochemical mechanisms occurring at these waves have not yet been established (work in progress). However, since here electrochemistry is used only for analytical purposes, only electron stoichiometries are of importance.

(25) Normalization of the current by its multiplication by $\theta^{1/2}$ allows us to correct the effects of diffusion. See *e.g.* ref 20, pp 142–143.

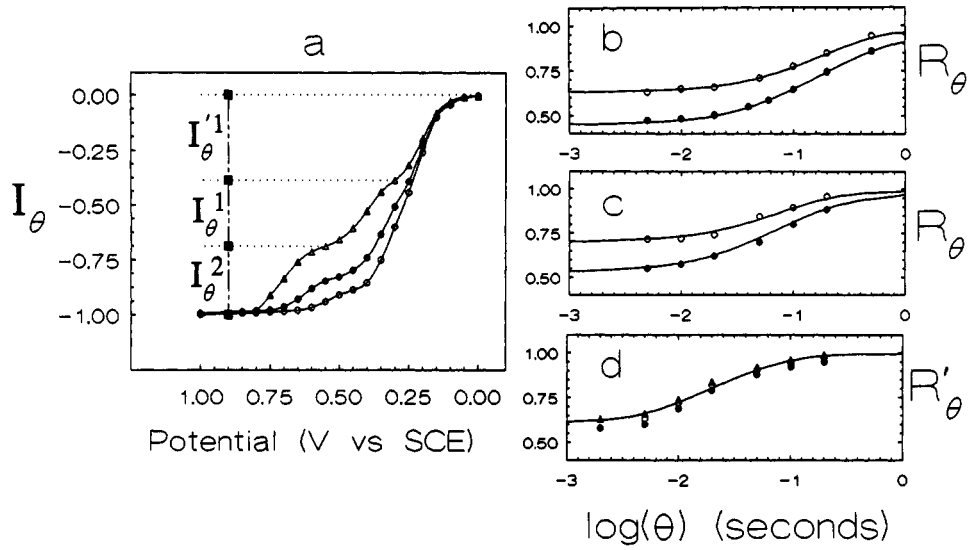

Figure 4. (a–c) Chronoamperometric oxidation of $Pd^0(dba)_2$ (2 mM) in the presence of various amounts of added PPh_3, in THF or DMF/*n*-Bu_4NBF_4 (0.3 M). (a) Variations of $I_\theta = [i_E(\theta)]\theta^{1/2}$, in THF, as a function of the pulse potential E. θ = 20 (△), 100 (●), and 200 ms (○). Note that I_θ values are given in normalized units to account for changes in electrode surface area. (b) Variations of $R_\theta = I_\theta^1/(I_\theta^1 + I_\theta^2)$ in DMF, as a function of the pulse duration θ and of the phosphine concentration. $[PPh_3]_0$ = 20 (●) and 40 mM (○). (c) Variations of $R_\theta = (I_\theta^1 + I_\theta'^1)/[(I_\theta^1 + I_\theta'^1) + I_\theta^2]$ in THF, as a function of the pulse duration θ and of the phosphine concentration. $[PPh_3]_0$ = 20 (●) and 40 mM (○). (d) Chronoamperometric oxidation of $Pd^0(PPh_3)_4$ (2 mM) in THF/*n*-Bu_4NBF_4 (0.3 M): variations of $R'_\theta = I_\theta'^1/(I_\theta^1 + I_\theta'^1)$ as a function of the pulse duration θ and of the phosphine concentration. $[PPh_3]_0$ = 20 (●), 30 (○), and 40 mM (△). Conditions: gold-disk electrodes (0.5-mm or 25-μm diameter); 20 °C. In b–d the solid curves are the predicted variations simulated on the basis of the pertinent rate laws and rate constants (see text).

overlapping of the two waves O_1 and O'_1. However, as shown by cyclic voltammetry, these latter waves concern only palladium(0) centers that do not bear a dba ligand, $Pd^0(dba)(PPh_3)_2$ being still oxidized at wave O_2 in THF. In agreement with this result, the variations of $R_\theta = (I_\theta^1 + I_\theta'^1)/[(I_\theta^1 + I_\theta'^1) + I_\theta^2]$, *viz.* of the sum $(I_\theta^1 + I_\theta'^1)$ of the currents observed at waves O_1 and O'_1 relative to the overall oxidation current $(I_\theta^1 + I_\theta'^1 + I_\theta^2)$, as a function of the potential step duration θ or of the phosphine concentration observed in THF (Figure 4c), parallel those described above in DMF (Figure 4b). Therefore, in THF a double equilibrium (*viz.* eqs 13 and 16), involving the three species $Pd^0(dba)(PPh_3)_2$, $Pd^0(PPh_3)_3$, and *S*–$Pd^0(PPh_3)_3$ must be considered instead of the single equilibrium existing in DMF between $Pd^0(dba)(PPh_3)_2$ and *S*–$Pd^0(PPh_3)_3$ (eq 13).

In agreement with our previous observations based on cyclic voltammetry, the variations of $R_\theta = I_\theta^1/(I_\theta^1 + I_\theta^2)$ in Figure 4b (or those of $R_\theta = (I_\theta^1 + I_\theta'^1)/[(I_\theta^1 + I_\theta'^1) + I_\theta^2]$, in Figure 4c) confirm that these equilibria are labile at longer times ($\theta \approx 1$ s), since R_θ tends toward unity, showing that all palladium(0) complexes may be oxidized at the potential of wave O_1 (or at that of O_1 and O'_1 in THF). Conversely, the equilibria are frozen at shorter times ($\theta \leq 5$ ms), and the value of R_θ then reflects the true equilibrium concentrations of $Pd^0(dba)(PPh_3)_2$ and *S*–$Pd^0(PPh_3)_3$ (or that of $Pd^0(dba)(PPh_3)_2$ *vis à vis* those of *S*–$Pd^0(PPh_3)_3$ and $Pd^0(PPh_3)_3$ in THF).[20,21]

The equilibrium between *S*–$Pd^0(PPh_3)_3$ and $Pd^0(PPh_3)_3$ in THF (eq 16) can be investigated more conveniently when the same method is applied to solutions of $Pd^0(PPh_3)_4$ in THF. Thus, the variations $R'_\theta = I_\theta'^1/(I_\theta^1 + I_\theta'^1)$, *viz.* of the relative oxidation currents at waves O_1 and O'_1, can be monitored as a function of the duration of the potential step θ and of the phosphine concentration. Such variations, represented in Figure 4d, evidence that this equilibrium is totally labile above a few tenths of a second but is "frozen" on the millisecond time scale. Moreover, it is noteworthy that R'_θ is almost independent of the phosphine concentration, a result that further confirms our above description of waves O_1 and O'_1 as featuring the oxidations of two species, with an identical number of phosphine ligands, *viz.* *S*–$Pd^0(PPh_3)_3$ and $Pd^0(PPh_3)_3$, related through a labile equilibrium (eq 16).

Reactivities of Mixtures of $Pd^0(dba)_2$, dba, and PPh_3 with PhI. Figure 1 presents the variations of the overall palladium(0) concentration with time when a few selected mixtures of $Pd^0(dba)_2$ and PPh_3 are reacted with excess PhI (5 equiv) in THF. These variations are determined by measuring the decay of the sum of the current plateaus of waves O_1 and O_2, *viz.* $(i^{lim}_{O_1} + i^{lim}_{O_2})/(i^{lim}_{O_1} + i^{lim}_{O_2})_{t=0}$, as measured with a rotating-disk electrode (RDE) whose potential is set on the plateau of wave O_2. It is noteworthy that identical results are obtained upon using $i^{lim}_{O_1}/(i^{lim}_{O_1})_{t=0}$, as determined when the potential of the RDE is set on the plateau of waves O_1 and O'_1. Such an identity is in complete agreement with our previous observation that on long time scales (*viz.* longer than a few seconds) such as those considered in Figure 1 (as evidenced by $t_{1/2}$ values) the equilibriums in eqs 13 and 16 are totally labile.

The same experiments were also performed in the presence of various excesses of dba and PPh_3. The variations of $(i^{lim}_{O_1} + i^{lim}_{O_2})/(i^{lim}_{O_1} + i^{lim}_{O_2})_{t=0}$ or of $i^{lim}_{O_1}/(i^{lim}_{O_1})_{t=0}$, similar to those reported in Figure 1, established that the overall rate of oxidative addition follows a kinetic law first order in zerovalent palladium and first order in PhI

$$d[\mathbf{Pd^0}]/dt = -k^{ap}([\mathbf{Pd^0}][PhI]) \qquad (17)$$

(where $[\mathbf{Pd^0}]$ represents the overall palladium concentration) where the apparent rate constant, k^{ap}, depends on the concentrations of free dba and PPh_3, as shown for

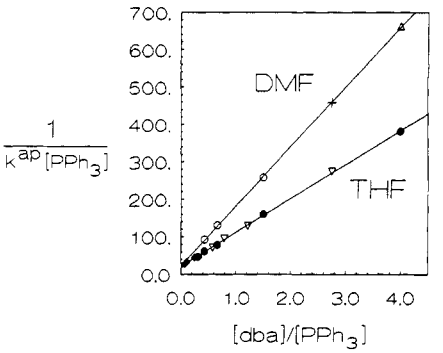

Figure 5. Variations of the apparent rate constant (k^{ap}, in $M^{-1}\cdot s^{-1}$, as defined in eq 17) of oxidative addition of PhI (5–20 equiv) to mixtures of $Pd^0(dba)_2$, dba, and PPh_3, as a function of dba and PPh_3 concentrations (in M)[26] in DMF/*n*-Bu_4NBF_4 (0.3 M) or in THF/*n*-Bu_4NBF_4 (0.3 M): initial concentration in $Pd^0(dba)_2$, C^0 = 2 mM; added concentration in PPh_3, $[PPh_3]_0$ = 10–80 mM; added concentration in dba, $[dba]_0$ = 0 (●), 20 (▽), and 40 mM (◆) in THF and $[dba]_0$ = 20 (○), 40 (+), and 60 mM (△) in DMF (20 °C).

example in Figure 5. Such data establish that k^{ap} obeys the variations[26]

$$1/k^{ap} = A[dba] + B[PPh_3] \quad (18)$$

where A and B are constants: A = 90.5 ± 0.5 s and B = 21.0 ± 0.5 s in THF (correlation coefficient 0.9997) and A = 159.5 ± 0.5 s and B = 22.1 ± 0.4 s in DMF (correlation coefficient 0.9999).

Discussion

The above results have established that when $Pd^0(dba)_2$ is dissolved in DMF in the presence of more than 2 equiv of PPh_3, the zerovalent palladium exists in two main forms, $Pd^0(dba)(PPh_3)_2$ and *S*-$Pd^0(PPh_3)_3$, which are in rapid equilibrium (eq 13) within the time scale of interest for oxidative addition. In THF, a poorer ligand, a third form exists, $Pd^0(PPh_3)_3$, which is also in equilibrium with the two previous ones (eq 16). In the following we wish to define further the thermodynamics and kinetics of these equilibria and explain their role in the overall reactivity of mixtures of $Pd^0(dba)_2$ and PPh_3 in oxidative-addition reactions.

The rate law in eqs 17 and 18 demonstrates that the reacting zerovalent palladium center involved in the true oxidative-addition elementary step is a species, present in the medium at steady-state concentration, that is in rapid equilibrium with the main species, *viz.* $Pd^0(dba)(PPh_3)_2$ and *S*-$Pd^0(PPh_3)_3$ (including also $Pd^0(PPh_3)_3$ in THF). One equilibrium involves a rapid and equilibrated deligation of dba and corresponds to the term $A[dba]$ in eq 18; another equilibrium, whose role is evidenced by the term $B[PPh_3]$ in eq 18, corresponds to the rapid deligation of PPh_3. Such requirements necessarily imply that the reacting species be *S*-$Pd^0(PPh_3)_2$, which formed by the equilibria

$$Pd^0(dba)(PPh_3)_2 \overset{S}{\rightleftarrows} S\text{-}Pd^0(PPh_3)_2 + dba \quad K_1 \quad (19)$$

$$S\text{-}Pd^0(PPh_3)_3 \rightleftarrows S\text{-}Pd^0(PPh_3)_2 + PPh_3 \quad K_2 \quad (20)$$

$$Pd^0(PPh_3)_3 \overset{S}{\rightleftarrows} S\text{-}Pd^0(PPh_3)_2 + PPh_3 \quad K_3 \quad (21)$$

$$S\text{-}Pd^0(PPh_3)_2 + PhI \rightarrow PhPd^{II}(PPh_3)_2I \quad k \quad (22)$$

Assuming that the reactive moiety *S*-$Pd^0(PPh_3)_2$ obeys steady-state conditions[4] and considering that the equilibria in eqs 19–21 remain always in equilibrium lead to a rate law identical with that in eq 17:[26]

$$1/k^{ap} = 1/k + (1/kK_1)[dba] + [(K_2 + K_3)/kK_2K_3][PPh_3] \quad (23)$$

Equation 23 agrees with the empirical laws observed in THF or DMF (eq 18) if, in both cases, $1/k$ is less than the experimental uncertainty, *viz.* $k \geq 20$ $M^{-1}\cdot s^{-1}$; then, $kK_1 = 1/A = (1.10 \pm 0.01) \times 10^{-2}$ s^{-1} and $kK_2K_3/(K_2 + K_3) = 1/B = (4.75 \pm 0.10) \times 10^{-2}$ s^{-1}, in THF and $kK_1 = (6.27 \pm 0.01) \times 10^{-3}$ s^{-1} and $kK_2K_3/(K_2 + K_3) = (4.6 \pm 0.4) \times 10^{-2}$ s^{-1} in DMF. Since only a minimum value can be estimated for k, only maximum values can be determined for K_1 ($\leq 5 \times 10^{-4}$ M in THF, $\leq 3 \times 10^{-4}$ M in DMF) and $K_2K_3/(K_2 + K_3)$ ($\leq 2.5 \times 10^{-3}$ M in THF, $\leq 2.5 \times 10^{-3}$ M in DMF). However, the value of $K_0 = K_1(K_2 + K_3)/K_2K_3 = B/A$ (*viz.* 0.232 ± 0.007 in THF and 0.140 ± 0.015 in DMF), which is the *pseudo*-equilibrium constant between $Pd^0(dba)(PPh_3)_2$ on the one hand and the sum of *S*-$Pd^0(PPh_3)_3$ and $Pd^0(PPh_3)_3$ on the other hand, can be determined with good accuracy:

$$Pd^0(dba)(PPh_3)_2 + PPh_3 \overset{S}{\rightleftarrows} \{Pd^0(PPh_3)_3, S\text{-}Pd^0(PPh_3)_3\} + dba \quad K_0 \quad (24a)$$

$$K_0 = \{([S\text{-}Pd^0(PPh_3)_3] + [Pd^0(PPh_3)_3])[dba]/([Pd^0(dba)(PPh_3)_2][PPh_3])\}_{equil} \quad (24b)$$

Besides the importance of K_0 in evaluating the nature of the main species present under given experimental conditions when $Pd^0(dba)_2$ is used in the presence of several equivalents (>2) of PPh_3, it is worth emphasizing that K_0 also allows us to compare the concentrations of the reactive moiety, *S*-$Pd^0(PPh_3)_2$, available under different conditions. For example, for identical overall concentrations of zerovalent palladium, the concentration of *S*-$Pd^0(PPh_3)_2$ in a solution of $Pd^0(PPh_3)_4$ (*i.e.* formally in a solution of $Pd^0(PPh_3)_3$ + 1 equiv of PPh_3) is $1/K_0$ (*i.e. ca.* 4.5) times larger than that present in a solution of $Pd^0(dba)(PPh_3)_2$ obtained by mixing 1 equiv of $Pd^0(dba)_2$ with 2 equiv of PPh_3 (*i.e.* formally $Pd^0(dba)(PPh_3)_2$ + 1 equiv of dba). Such an order of magnitude is in good agreement with the respective values of the half-lives determined in Figure 1; for example, in THF $t_{1/2} \approx 3.5 \pm 0.5$ s for $Pd^0(PPh_3)_4$ and $t_{1/2} = 20 \pm 1$ s for the mixture of $Pd^0(dba)_2$ with 2 equiv of PPh_3.

This determination of K_0, based on the treatment of kinetics of the oxidative addition of PhI with solutions of $Pd^0(dba)_2$ in the presence of dba or PPh_3, can be independently confirmed by the results of chronoamperometric measurements such as those presented in Figure 4b,c. Indeed, the limits observed for R_Θ at short times represent the relative equilibrium concentrations of *S*-$Pd^0(PPh_3)_3$ (in DMF, Figure 4b, or of the sum of equilibrium concentrations of $Pd^0(PPh_3)_3$ and *S*-$Pd^0(PPh_3)_3$, in THF,

(26) In the plot presented in Figure 5 or in eq 18, the concentrations of phosphine or dba are the concentrations of the free ligands. The best correlation was obtained by considering that $[dba] = [dba]_0 + 2C^0$ and $[PPh_3] = [PPh_3]_0 - 2C^0$, where $[dba]_0$ and $[PPh_3]_0$ are the respective concentrations of dba and phosphine *added* to the solution of $Pd^0(dba)_2$ at initial concentration C^0 in palladium(0). Such formulations are fully consistent with the values of K_0 (eqs 24a,b) and the mechanism in Scheme I (*vide infra* and Experimental Section).

Figure 4c) *vis à vis* the overall zerovalent palladium concentration (P = PPh_3):

$$\lim_{\theta\to 0} R_\theta = \{([S\text{-}Pd^0P_3] + [Pd^0P_3])/([S\text{-}Pd^0P_3] + [Pd^0P_3] + [Pd^0(dba)P_2])\}_{equil} \quad (25)$$

that is

$$K_0 = \{\lim_{\theta\to 0} R_\theta/(1 - \lim_{\theta\to 0} R_\theta)\}([dba]/[PPh_3])_{equil} \quad (26)$$

where K_0 is defined in eq 24b. Treatment of data such as those presented in Figure 4b,c affords $(K_0)_{DMF} = 0.16 \pm 0.02$ and $(K_0)_{THF} = 0.23 \pm 0.03$, these values being in very good agreement with those found independently on the basis of kinetics of oxidative addition (respectively 0.140 ± 0.015 and 0.232 ± 0.007; *vide supra*).

To conclude this section about thermodynamic aspects, let us consider the equilibrium in eq 16 that relates $Pd^0(PPh_3)_3$ and S-$Pd^0(PPh_3)_3$ in THF. From the short-time limit of the chronoamperometric data shown in Figure 4d, one may evaluate the relative equilibrium concentration of the species oxidized at wave O'_1, *vis à vis* the overall zerovalent palladium concentration, in mixtures of $Pd^0(PPh_3)_4$ and PPh_3. However, it is impossible for us to decide on an absolute basis whether THF-$Pd^0(PPh_3)_3$ or $Pd^0(PPh_3)_3$ is oxidized at wave O'_1. By analogy with what is observed in the presence of added DMF (compare Figure 3e), *viz.* that coordination of DMF results in a negative shift of the oxidation potential of the palladium(0) center, we are inclined to consider that wave O'_1 represents the oxidation of THF-$Pd^0(PPh_3)_3$. On the basis of this assumption,[27] one has (P = PPh_3)

$$\lim_{\theta\to 0} R'_\theta = \{[THF\text{-}Pd^0P_3]/([THF\text{-}Pd^0P_3] + [Pd^0P_3])\}_{equil} \quad (27)$$

that is, for eq 16

$$K_S = K_3/K_2 = ([THF\text{-}Pd^0P_3]/[Pd^0P_3])_{equil} = \{\lim_{\theta\to 0} R_\theta/(1 - \lim_{\theta\to 0} R_\theta)\} \quad (28)$$

Treatment of the data in Figure 4d affords $(K_S)_{THF} = 1.45 \pm 0.15$;[27] note that $(K_S)_{DMF} \gg 1$, since a single oxidation wave (*viz.* that of DMF-$Pd^0(PPh_3)_3$) is observable in DMF.

Let us now focus on the dynamic aspects of these equilibria. From the ^{31}P data we know that the doublet characterizing $Pd^0(dba)(PPh_3)_2$ is well resolved, and its position is independent of the dba or phosphine excess. This shows that any equilibrium in which this species participates is frozen within the short time scales of NMR. Conversely, a single broad signal, whose position is highly dependent on the phosphine excess, features the resonance of PPh_3 or PPh_3 ligated to those palladium(0) centers that do not contain a dba ligand. This means that these latter species are co-involved in some rapid equilibria that are fully dynamic within the time scale of NMR.

From the transient electrochemical data one may observe the dynamic behavior of some of these equilibria within a much larger time scale (between 1 ms and 1 s). Let us first consider the equilibrium in eq 16 in THF. The variations of R'_θ in Figure 4d feature the progressive "freezing" of the equilibrium between $Pd^0(PPh_3)_3$ and S-$Pd^0(PPh_3)_3$ when the time scale is decreased from 1 s to 1 ms. This interpretation is further substantiated by the good fit between the theoretical prediction (solid line) and the experimental data shown in Figure 4d. From this fit the rate constant $k_S = 26 \pm 3\ s^{-1}$ is determined for the forward reaction in eq 16, from where it follows that the backward rate constant is $k_{-S} = k_S/K_S = 18 \pm 3\ s^{-1}$. If such values are sufficiently large for the equilibrium in eq 16 to be considered as infinitely rapid *vis à vis* the rate of oxidative addition (*vide supra*), they are too small to account for the fact that $Pd^0(PPh_3)_3$, THF-$Pd^0(PPh_3)_3$, and PPh_3 gives a single broad signal in ^{31}P NMR. This suggests that the coalescence is due to the participation of other equilibria (presumably those in eqs 4, 20, and 21) that must be fast enough at 20 °C to be labile within the NMR time scale.

The dynamics of the equilibria between $Pd^0(dba)(PPh_3)_2$ and S-$Pd^0(PPh_3)_3$ (including also $Pd^0(PPh_3)_3$ in THF) in eq 13 may be studied according to the same lines from the variations of R_θ in Figure 4b,c. In both solvents (THF or DMF) these data could not be represented by a kinetic model based on the reaction orders corresponding to the formulation of the stoichiometric eq 13. Oppositely good fits were obtained in both solvents when we considered that the forward reaction was first order in $Pd^0(dba)(PPh_3)_2$ and zero order in phosphine or in dba, whereas the backward reaction was first order in S-$Pd^0(PPh_3)_3$ (or in the sum of $Pd^0(PPh_3)_3$ and S-$Pd^0(PPh_3)_3$, in THF), first order in dba, and −1 reaction order in phosphine, *i.e.*

$$d[Pd^0(dba)(PPh_3)_2]/dt = -k_+[Pd^0(dba)(PPh_3)_2] - k_-([dba]/[PPh_3])(C^0 - [Pd^0(dba)(PPh_3)_2]) \quad (29)$$

where C^0 is the total initial zerovalent palladium concentration introduced in the cell. Such a peculiar rate law establishes that eq 13 does not represent an elementary step but results from the combination of at least two processes. The experimental reaction orders are consistent with a formulation such as that in eqs 30 and 31 (completed by eq 32 in THF), where eq 31 (and also eq 32 in THF)

$$Pd^0(dba)(PPh_3)_2 \overset{S}{\rightleftarrows} S\text{-}Pd^0(PPh_3)_2 + dba \quad \text{forward, } k_f\text{; backward, } k_b \quad (30)$$

$$S\text{-}Pd^0(PPh_3)_2 + PPh_3 \rightleftarrows S\text{-}Pd^0(PPh_3)_3 \quad 1/K_2 \quad (31)$$

$$S\text{-}Pd^0(PPh_3)_3 \overset{S}{\rightleftarrows} Pd^0(PPh_3)_3 \quad 1/K_S \quad (32)$$

are fast equilibria (within the time scale considered here), the rate-determining step being eq 30. Since we know that S-$Pd^0(PPh_3)_2$ is a transient intermediate present only at trace levels under our conditions,[4] its concentration can be neglected in the conservation equation for palladium(0). The sequence in eqs 30–32 is then easily shown to obey the rate law

$$d[Pd^0(dba)(PPh_3)_2]/dt = -k_f[Pd^0(dba)(PPh_3)_2] + [k_bK_2K_S/(1 + K_S)]([dba]/[PPh_3])(C^0 - [Pd^0(dba)(PPh_3)_2]) \quad (33)$$

which is identical with the experimental rate law in eq 29, if $k_+ = k_f$ and $k_- = k_bK_2K_S/(1 + K_S)$. Note that, in DMF,

(27) If the attribution is incorrect (*i.e.* if O_1 and O'_1 were to feature respectively the oxidations of THF-$Pd^0(PPh_3)_3$ and $Pd^0(PPh_3)_3$, instead of those of $Pd^0(PPh_3)_3$ and THF-$Pd^0(PPh_3)_3$, as assumed in the text), $1/(K_S)_{THF}$ is determined instead. Note that since the value of $(K_S)_{THF}$ is found to be close to unity, the consequences of a possible error in this attribution are small. In particular the value of K_0 is not affected.

Table I. Rate and Equilibrium Constants Describing the Composition and Apparent Overall Reactivity of Mixtures of $Pd^0(dba)_2$ and PPh_3, at 20 °C, in THF or in DMF

reacn[a]	solvent	$k_{forward}$ (s^{-1})	$k_{backward}$	K_{eq}
$Pd^0(dba)P_2 \overset{S}{\rightleftarrows} S\text{-}Pd^0P_2 + dba$	DMF	5.1 ± 0.6	$\geq 2 \times 10^4$ $M^{-1}\cdot s^{-1}$	$\leq 3 \times 10^{-4}$ M
	THF	10 ± 1	$\geq 10^4$ $M^{-1}\cdot s^{-1}$	$\leq 5 \times 10^{-4}$ M
$S\text{-}Pd^0P_3 \overset{S}{\rightleftarrows} S\text{-}Pd^0P_2 + PPh_3$	DMF	*b*	*b*	$\leq 2.5 \times 10^{-3}$ M
	THF	*b*	*b*	$\leq 4 \times 10^{-3}$ M
$Pd^0(dba)P_2 + PPh_3 \overset{S}{\rightleftarrows} S\text{-}Pd^0P_3 + dba$[c]	DMF	5.1 ± 0.6	32 ± 7 s^{-1}	0.140 ± 0.015
	THF	10 ± 1	105 ± 15 s^{-1}	0.14 ± 0.01
$Pd^0P_3 \overset{S}{\rightleftarrows} S\text{-}Pd^0P_3$[d]	THF	26 ± 3	18 ± 3 s^{-1}	1.45 ± 0.15
$Pd^0(dba)P_2 + PhI \rightarrow Ph\text{-}Pd^{II}P_2I + dba$[e]	DMF	$(6.27 \pm 0.01) \times 10^{-3}$		
	THF	$(1.10 \pm 0.1) \times 10^{-2}$		
$S\text{-}Pd^0P_3 + PhI \rightarrow Ph\text{-}Pd^{II}P_2I + PPh_3$[f]	DMF	$(4.6 \pm 0.4) \times 10^{-2}$		
	THF	$(4.75 \pm 0.10) \times 10^{-2}$		

[a] P = PPh_3. [b] Too fast to be determinable; labile within the time scale of ^{31}P NMR (162 MHz). [c] Not an elementary step; $k_{forward}$ and $k_{backward}$ correspond to the apparent rate law $d[Pd^0(dba)P_2]/dt = -k_{forward}[Pd^0(dba)P_2] + k_{backward}[S\text{-}Pd^0P_3][dba]/[PPh_3]$. [d] $K \gg 1$ in DMF. [e] Not an elementary step; $k_{forward}$ is an apparent rate constant corresponding to the overall rate law $d[Pd^0]/dt = -k_{forward}[Pd^0][PhI]/[L]$, with $[Pd^0]$ = total concentration in zerovalent palladium complexes and L = dba. [f] As for footnote *e*, except L = PPh_3.

Table II. Experimental and Predicted Rate Constants, k_{exp}, and Half-Reaction Times, $t_{1/2}$, for Oxidative Addition of PhI to the Different Systems Considered in Figure 1, at 20 °C[a]

conditions[a]		$10^2 k_{exp}$ (s^{-1})[b]		$t_{1/2}$ (s)[c]	
system	solvent	exptl	predicted	exptl	predicted
$Pd^0(PPh_3)_4$	DMF	5.4 ± 0.2	4.6 ± 0.4	3.5 ± 0.5	4.1 ± 0.4
	THF	5.1 ± 0.4	4.8 ± 0.1	3.5 ± 0.5	4.0 ± 0.1
$Pd^0(dba)_2 + PPh_3$ (2 equiv)	DMF	0.63 ± 0.03	0.63	32 ± 2	30
	THF	0.94 ± 0.05	1.10	20 ± 2	17
$Pd^0(dba)_2 + PPh_3$ (4 equiv)	DMF	0.63 ± 0.02[d]	0.63[d]	40 ± 2	37[d]
	THF	0.93 ± 0.05[d]	1.10[d]	26 ± 2	24[d]

[a] Total concentration in zerovalent palladium complexes: 2 mM; [PhI] = 10 mM. [b] k_{exp} corresponds to the rate laws in eqs 34 and 36, respectively (see text) with $\gamma = 5$. [c] Predicted $t_{1/2}$ values are evaluated from eqs 35 and 37, respectively (see text) with $\gamma = 5$, using the predicted value of k_{exp}. [d] Using $(K_0)_{DMF} = 0.15$ or $(K_0)_{THF} = 0.23$, in eqs 36 or 37, respectively. Uncertainties for predicted values are given only when they affect the last digit shown.

$K_S \gg 1$ and therefore $k_- = k_b K_2$. From the experimental values of k_+ and k_- measured in both solvents, one obtains $(k_f)_{DMF} = 5.1 \pm 0.6$ s^{-1}, $(k_b K_2)_{DMF} = 32 \pm 7$ s^{-1} and $(k_f)_{THF} = 10 \pm 1$ s^{-1}, $(k_b K_2)_{THF} = 105 \pm 15$ s^{-1}. The solid lines fitting the data in Figure 4b,c are determined from the rate law in eq 33 with the above set of values, and $K_S = 1.45 \pm 0.15$ in THF or $[K_S/(1 + K_S)] = 1$ in DMF (*viz.* $K_S \gg 1$), as independently determined above.

The above series of results establishes that the reactivity of mixtures of $Pd^0(dba)_2$ and PPh_3 (2 equiv at least) *vis à vis* oxidative-addition reactions needs to be described by the whole set of reactions represented in Scheme I. The various rate and equilibrium constants describing the above reactions are summarized in Table I for both solvents investigated (THF and DMF). From these data and Scheme I, the reactivity of each system considered in Figure 1 can be predicted and compared to the experimental results. Oxidative additions of PhI (γ equivalents; $\gamma > 1$) to a mixture of $Pd^0(dba)_2$ with 2 equiv of PPh_3, or to $Pd^0(PPh_3)_4$, obey the rate law

$$(\gamma + 1)\ln[(\gamma + x - 1)/\gamma] - 2\ln x = k_{exp}(\gamma - 1)t \quad (34)$$

where x is the fraction of the overall unconverted zerovalent palladium, $x = [\mathbf{Pd^0}]/[\mathbf{Pd^0}]_{t=0}$, and k_{exp} is an apparent rate constant whose value depends on the system used: $k_{exp} = kK_1$ for $Pd^0(dba)_2$ with 2 equiv of PPh_3 and $k_{exp} = kK_2K_3/(K_2 + K_3)$ for $Pd^0(PPh_3)_4$, where k, K_1, K_2, and K_3 are the rate and equilibrium constants defined respectively in eqs 22, 19, 20, and 21. The solid lines fitting the experimental data presented in Figure 1 are determined according to the rate law in eq 34. The resulting values of k_{exp} are reported in Table II (third column) with the experimental half-lives, $t_{1/2}$, measured for the conditions of Figure 1 (fifth column). Both sets of values are compared in the same table to their values predicted (fourth and sixth columns, respectively) on the basis of the above results, $t_{1/2}$ being deduced as follows from eq 34:

$$t_{1/2} = \{(\gamma + 1)\ln[(\gamma - 0.5)/\gamma] + 2\ln 2\}/[(\gamma - 1)k_{exp}] \quad (35)$$

The same treatment was applied to the kinetics of oxidative addition of PhI to the mixture of $Pd^0(dba)_2$ with 4 equiv of PPh_3, which is also presented in Figure 1. The corresponding rate law and half-life are then given as

$$(\gamma + 1 + 2K_0)\ln[(\gamma + x - 1)/\gamma] - 2(1 + K_0)\ln x = k_{exp}(\gamma - 1)t \quad (36)$$

$$t_{1/2} = \{(\gamma + 1 + 2K_0)\ln[(\gamma - 0.5)/\gamma] + 2(1 + K_0)\ln 2\}/[(\gamma - 1)k_{exp}] \quad (37)$$

where $k_{exp} = kK_1$ and k, K_1, and K_0 are defined respectively in eqs 22, 19, and 24. The solid lines fitting the experimental data shown in Figure 1 for $Pd^0(dba)_2$ with 4 equiv of PPh_3 are based on the theoretical law in eq 36, with k_{exp} as given in Table II.

Scheme I

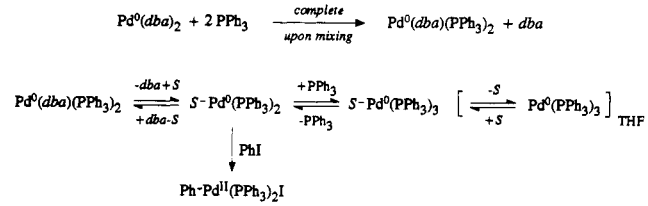

Conclusions

The above study has shown that preparation *in situ* of zerovalent palladium catalysts by mixing $Pd^0(dba)_2$ with several equivalents (≥2) of phosphine results in systems more complex than usually thought by the precursors of this method. Indeed, to deligate completely dba from the palladium center 6–8 equiv of phosphine, depending on the solvent, are required at least. This could be a serious problem for the method when the phosphine is expensive, for example when chiral species are used.[10i,l,m,s,t] Indeed, by comparison to the direct use of $Pd^0(PR_3)_4$, the method appears *a priori* to require larger excesses of phosphine if dba-coordinated palladium species are undesirable.

However, this conclusion is valid only for what concerns the thermodynamic (*viz.* static) composition of the solution. In terms of reactivity, *viz.* with respect to oxidative addition, the conclusion is quite opposite. Indeed, when at least 2 equiv of phosphine is used per equivalent of $Pd^0(dba)_2$, oxidative addition proceeds through the same intermediate that is involved in oxidative additions to $Pd^0(PPh_3)_4$. It is worth emphasizing that, although the main zerovalent palladium species present in the medium may be $Pd^0(dba)(PPh_3)_2$, the active form of the catalyst, *viz.* the low-ligated zerovalent palladium transient complex S-$Pd^0(PPh_3)_2$, contains two phosphine ligands and no dba.

Therefore, in terms of steric or electronic effects in the activated complex of oxidative addition, using $Pd^0(dba)_2$ and 2 equiv of phosphine or using $Pd^0(PPh_3)_4$ should lead to equivalent results. From a synthetic point of view, the first system then appears preferable for expensive phosphines. However, this gain is earned at the expense of a decrease in the overall reactivity of the system, as illustrated in Figure 1. As explained above, it must be emphasized that this decrease of reactivity (by a factor of *ca.* 4.5) does not stem from differences in activated complexes but reflects a decrease of the steady-state concentration of the key intermediate S-$Pd^0(PPh_3)_2$. This originates from the fact that, in contradiction with previous statements,[28] dba is a better ligand than PPh_3 for the S-$Pd^0(PPh_3)_2$ moiety, as apparent in the small values of K_0 (eq 24) in both solvents considered in this study.

Experimental Section

Chemicals. THF (Janssen) was stored over potassium hydroxide for 24 h and distilled from a sodium benzophenone solution under an argon atmosphere before use. DMF (Janssen) was distilled over CaH_2 under vacuum and stored under an argon atmosphere before use. Both solvents were transferred to the cells according to standard Schlenk procedures. n-Bu_4NBF_4 was obtained from the hydrogen sulfate salt (Janssen), by treatment with $NaBF_4$ (Janssen) in water. It was further recrystallized from ethyl acetate/petroleum ether, dried under vacuum, and stored under argon before use.

Bis(dibenzylideneacetone)palladium(0),[29] tetrakis(triphenylphosphine)palladium(0),[30] and *trans*-(σ-C_6H_5)$Pd(PPh_3)_2I$[31] were synthesized according to published procedures.

^{31}P and ^1H NMR. ^1H NMR spectra were performed in d_8-THF on a Bruker AC 250-MHz spectrometer using TMS as the internal reference. ^{31}P NMR spectra were performed in THF or in DMF on a Bruker 162-MHz spectrometer using H_3PO_4 as an external reference.

Electrochemical Setup and Electrochemical Procedures. Cyclic voltammetry and chronoamperometry were performed as described in previous works of this group.[8] Electrodes consisted of gold disks of 0.5-mm or 25-μm diameters that were selected as a function of scan rate or pulse duration to minimize the ohmic drop without edge effects.[32] A home-built potentiostat equipped with positive feedback for ohmic-drop compensation was used.[33] The reference electrode was an SCE (Tacussel) separated from the solution by a bridge (3 mL) filled with a 0.3 M n-Bu_4NBF_4 solution in THF or DMF, identical with that used in the cell. All potentials given here refer to this reference electrode. All the experiments reported here were performed at 20 °C (Lauda RC20 thermostat). All data were stored using a Nicolet 391 digital oscilloscope and transferred to a PC-386 computer (Amstrad) for treatment and presentation of the results.

Kinetics such as those represented in Figures 1 and 5 were followed using a rotating-gold-disk electrode of 2-mm diameter (Tacussel), whose potential was continuously imposed on the plateau of the wave selected (*viz.* either O_1 or O_2, see text). The variations of the disk current as a function of time were recorded by a Nicolet 391 digital oscilloscope and transferred to a PC-386 computer for treatment and presentation of the results.

Electron consumptions in transient electrochemistry were determined by following a method previously described that combines the use of classical working electrodes and ultramicroelectrodes.[24b] Other electrochemical procedures are identical with those previously described.[8]

Simulations of the Working Curves. The working curves used in this study were simulated according to classical explicit finite difference procedures as described previously for similar CE mechanisms.[34]

Derivation of Rate Laws. Equation 23 is obtained by considering that because of the fast equilibria in eqs 19–21:

$$[S\text{-}Pd^0(PPh_3)_2] = [\mathbf{Pd^0}]/\{1 + [dba]/K_1 + [PPh_3]/K_2 + [PPh_3]/K_3\}$$

Therefore, from eq 22:

$$d[\mathbf{Pd^0}]/dt = -k([S\text{-}Pd^0(PPh_3)_2][PhI]) = -(k/\{1 + [dba]/K_1 + [PPh_3]/K_2 + [PPh_3]/K_3\})([\mathbf{Pd^0}][PhI])$$

Comparison of this formulation with that in eq 17 shows readily that k^{ap} is given by eq 23.

The other rate laws were derived by following classical integration rules. However, to achieve compact analytical forms such as those given in the text for the expressions in eqs 34 and 35 or in eqs 36 and 37 approximations were required to evaluate the concentration of free dba or free PPh_3 present in the medium. For this, the true concentrations were determined rigorously on the basis of the equilibrium in eq 24a and conservation of matter equations. Thus, for any of the systems considered in this study, the instant concentrations of dba and phosphine are shown to obey the following set of coupled relationships:

$$[dba] = [dba]_0 + 2C^0 - [\mathbf{Pd^0}]\{[dba]/([dba] + K_0[PPh_3])\}$$

$$[PPh_3] = [PPh_3]_0 - 2C^0 - [\mathbf{Pd^0}]\{K_0[PPh_3]/([dba] + K_0[PPh_3])\}$$

(28) (a) See *e.g.*: Maitlis, P. M.; Espinet, P.; Russell, M. J. H. In *Comprehensive Organometallic Chemistry*; Wilkinson, G., Stone, F. G. A., Abel, E. W., Eds.; Pergamon Press: New York, 1982; Vol. 6, Chapter 38.2, p 260. (b) *Ibid.*, Vol. 6, Chapter 38.6, p 370.

(29) (a) Takahashi, Y.; Ito, T.; Sakai, S.; Ishii, Y. *J. Chem. Soc. D* **1970**, 1065. (b) Rettig, M. F.; Maitlis, P. M. *Inorg. Synth.* **1977**, *17*, 134.

(30) (a) Hartley, F. *Organomet. Chem. Rev., Sect. A* **1970**, *6*, 119. (b) Rosevear, D. T.; Stone, F. G. *J. Chem. Soc. A* **1968**, 164.

(31) (a) Fitton, P.; Johnson, M. P.; McKeon, J. E. *J. Chem. Soc. D* **1968**, 6. (b) Fitton, P.; Rick, E. A. *J. Organomet. Chem.* **1971**, *28*, 287.

(32) (a) Wipf, D. O.; Wightman, R. M. In *Electroanalytical Chemistry*; Bard, A. J., Ed.; Dekker: New York, 1989; Vol. 15, p 267–353. (b) Amatore, C.; Lefrou, C. *Port. Electrochim. Acta* **1991**, *9*, 311.

(33) Amatore, C.; Lefrou, C.; Pflüger, F. *J. Electroanal. Chem. Interfacial Electrochem.* **1989**, *270*, 43.

(34) Lee, K. Y.; Amatore, C.; Kochi, J. K. *J. Phys. Chem.* **1991**, *95*, 1285.

from which it follows

$$[\text{dba}] + [\text{PPh}_3] = [\text{dba}]_0 + [\text{PPh}_3]_0 - [\mathbf{Pd^0}]$$

where $[\mathbf{Pd^0}]$ is the instant overall concentration in zerovalent palladium complexes. Whenever dba or the phosphine are in large excess *vis à vis* the palladium(0), that is under the conditions of Figure 5 and eqs 17, 18, and 23, it follows that $[\text{dba}] \approx [\text{dba}]_0 + 2C^0$ and $[\text{PPh}_3] \approx [\text{PPh}_3]_0 - 2C^0$. Therefore, the experimental data obtained under these conditions (Figure 5) were processed on the basis of these approximations; similarly, the rate law in eq 23 was derived by considering these approximations. The resulting errors introduced in the treatment of data are less than 1%, *i.e.* much less than that on the experimental data.

For the conditions where eq 36 applies ($[\text{dba}]_0 = 0$, $[\text{PPh}_3]_0 = 4C^0$), complete resolution of the above set of equations shows that $[\text{PPh}_3]/C^0 = 1.8$, 1.9, and 2.0 for $[\mathbf{Pd^0}]/C^0 = 1.0$, 0.5, and 0.0, respectively. Owing to the small magnitude of K_0 and to its accuracy, $[\text{PPh}_3]$ was considered as equal to $2C^0$ irrespective of the advancement of the reaction. This led to $[\text{dba}] = 2C^0 - [\mathbf{Pd^0}]$, which was therefore used for the derivation of the rate law in eq 36. The resulting error introduced is less than 2%, *i.e.* much less than that on the experimental data.

Acknowledgment. This work has been supported in part by the CNRS (URA 1110 Activation Moléculaire) and by the ENS.

OM930241Y